

Model for Ferromagnetic Quantum Critical Point in a 1D Kondo Lattice

Yashar Komijani¹ and Piers Coleman^{1,2}

¹*Department of Physics and Astronomy, Rutgers University, Piscataway, New Jersey, 08854, USA*

²*Department of Physics, Royal Holloway, University of London, Egham, Surrey TW20 0EX, UK*

(Dated: December 14, 2024)

Motivated by recent experiments, we study a quasi-one dimensional model of a Kondo lattice with Ferromagnetic coupling between the spins. Using bosonization and dynamical large- N techniques we establish the presence of a Fermi liquid and a magnetic phase separated by a local quantum critical point, governed by the Kondo breakdown picture. Thermodynamic properties are studied and a gapless charged mode at the quantum critical point is highlighted.

INTRODUCTION

Heavy fermion materials are a class of quantum system in which the close competition between magnetism and itineracy drives a wealth of novel quantum ground states, including hidden order, strange and quantum critical metals, topological insulators and unconventional superconductivity [1, 2]. The various entanglement mechanisms by which the localized magnetic moments correlate and transform heavy fermion materials provide an invaluable window on the governing principles needed to control and manipulate quantum matter.

An aspect of particular interest is the quantum criticality that develops when a second-order magnetic phase transition is tuned to absolute zero. In weakly interacting materials, such magnetic quantum critical points can be understood as variants on the classic Slater-Stoner instabilities of Fermi liquids (FLs), described by the interaction of soft magnons with a Fermi surface according to the Hertz-Millis-Moriya theory [3–5]. The nature of quantum criticality in strongly interacting materials, in which the magnetism has a localized moment character, is less well understood, but is thought to involve a partial or complete Mott localization of the electrons, which in heavy fermion compounds manifests itself as the break-down of the Kondo effect and a possible collapse in the Fermi surface volume [6–9].

Most research into heavy fermion quantum criticality has focused on antiferromagnetic instabilities, often discussed as a competition between the Kondo screening of local moments, and antiferromagnetism, driven by the Ruderman-Kittel-Kasuya-Yosida (RKKY) interaction [10–12]. However, there is now a growing family of heavy-fermion systems, including α and β -YbAlB₄ [13–15], YbNi₄P₂ [16], YbNi₃Al₉ [17] and CeRu₂Al₂B [18], in which the interplay of the Kondo effect and ferromagnetism is involved in the quantum criticality [19].

Motivated by these discoveries here we examine quantum criticality in a Kondo lattice with ferromagnetic interactions. A ferromagnetic Kondo lattice affords many simplifications, for the uniform magnetization M of a Kondo lattice commutes with the Hamiltonian $[M, H] = 0$ and is thus a conserved quantity, free from quantum zero-point motion. Antiferromagnetic Kondo lattices are normally discussed in terms of a “generalized” two-dimensional phase diagram [6, 8] with

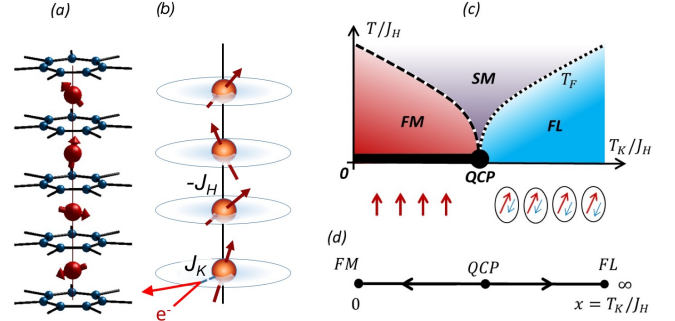


FIG. 1. (a) The quasi-1D structure of Yb local moments (red) in YbAlB₄ sandwiched between conducting B layers. (b) 1D model, showing local moments (orange), coupled via a ferromagnetic coupling $-J_H < 0$, each Kondo-coupled to a separate conduction electron sea via a coupling constant of strength J_K (white-blue layers). (c) Phase diagram we find for the model as a function of $x = T_K/J_H$ and temperature, showing Fermi liquid and 1D ferromagnetic regime, separated by a QCP. The Fermi temperature of the FL, T_F vanishes at the QCP. The 1D FM only orders at zero temperature and is intrinsically quantum critical. (d) RG flow of transverse Ising model to which our model maps in the Ising limit.

two axes - the Doniach parameter $x = T_K/J_H$, set by the ratio of the Kondo temperature T_K to the Heisenberg coupling J_H and the frustration parameter (y) measuring the strength of magnetic zero point fluctuations. The elimination of magnetic zero point fluctuations allows us to focus purely on the x -axis of the generalized phase diagram. Moreover, it now becomes possible to study magnetic quantum criticality in a one dimensional model.

Our model is motivated by the quasi-one dimensional Yb structure of YbAlB₄, in which a chain of ferromagnetically coupled Yb spins hybridizes with multiple conducting planes of B atoms (Fig. 1.) [20]. For simplicity, we treat each plane as an autonomous electron bath, individually coupled via an antiferromagnetic Kondo coupling J_K , according to

$$H = \sum_j \left(H_c(j) + J_K \vec{S}_j \cdot \vec{\sigma}_j - J_H \vec{S}_j \cdot \vec{S}_{j+1} \right), \quad (1)$$

where \vec{S}_j is the spin at the j -th site, coupled ferromagnetically to its neighbor with strength J_H . $H_c(j) =$

$\sum_{\mathbf{p}} \epsilon_{\mathbf{p}} c_{\mathbf{p}\alpha}^\dagger(j) c_{\mathbf{p}\alpha}(j)$ describes the j -th layer of electrons, coupled to the chain via its spin density $\vec{\sigma}_j = \psi_{j\alpha}^\dagger \vec{\sigma}_{\alpha\beta} \psi_{j\beta}$ at the chain, where \mathbf{p} is the momentum of the conduction electrons at the j -th layer and $\psi_{j\alpha}^\dagger = \sum_{\mathbf{p}} c_{\mathbf{p}\alpha}^\dagger(j)$ creates an electron at the position of impurity site on the chain.

The physics of this model is determined by the ratio $x = T_K/J_H$. At small x the 1D chain is ferromagnetically correlated, developing true long range order only at zero temperature, while at large x it forms a paramagnet where each spin is individually screened: in between, there is a quantum critical point (QCP) [10, 19]. We can explicitly demonstrate this QCP in the Ising limit of this Kondo lattice at the Toulouse decoupling point [21, 22], which permits bosonization of the Hamiltonian, mapping it [23] onto the transverse field Ising model, $H \rightarrow T_K \sum_n S_n^x + J_H^z \sum_n S_n^z S_{n+1}^z$. This model has a well-known RG flow [Fig. 1(d)] and a quantum phase transition at $J_H^z = T_K$ [24]. However, in this limit, the stable phases are gapped and to gain a deeper insight into the physics of the QCP, we return to the Heisenberg limit.

Earlier work on the ferromagnetic Kondo lattice has employed a long-wavelength description of the magnons [19]. Here instead, we use a large- N Schwinger boson approach which treats the magnetism, while also explicitly preserving the Kondo effect. Our method unifies the Arovas and Auerbach treatment of ferromagnetism [25] with the description of the Kondo problem by Parcollet, Georges et al [26–29]. An important aspects of this approach, is the use of a multi-channel Kondo lattice in which the spin S and the number of channels K is commensurate ($K = 2S$), allowing for a perfectly screened Kondo effect [29].

Figure 1(c) summarizes the key results of our study. At large $x = T_K/J_H$ our method describes a FL phase with Pauli susceptibility $\chi \sim 1/T_F$ and a linear specific heat coefficient $\gamma = C/T \sim 1/T_F$. As x is reduced to a critical value x_c , the characteristic scale $T_F(x)$ drops to zero, as indicated by the suppression of the characteristic temperature scale of the magnetic susceptibility and linear specific heat coefficient (Fig. 2 (c,d)). Curiously, the mechanism of suppression bears close resemblance to the Schrieffer mechanism for the reduction of the Kondo temperature in Hund's metals [30–33], and we find that $T_F(x)$ goes continuously to zero, terminating at a QCP $x = x_c$. The large N QCP is characterized by powerlaw dependences of the specific heat, local and uniform susceptibilities.

$$\chi(T) \sim \frac{1}{T}, \quad \chi_{loc}(T) \sim \frac{1}{T^{1-\alpha}}, \quad \frac{C}{T} \sim \frac{1}{T^\alpha} \quad (2)$$

where the exponent $\alpha[s] < 1$ is function of the spin $s = 2S/N$. At still smaller x the chain develops a fragile Ferromagnetism which disappears at finite temperatures. Here $\chi \sim 1/T^2$ and $C/T \sim 1/\sqrt{T}$ characteristics of a critical 1D Ferromagnetism (FM). There are two notable aspects of the physics: first, the QCP exhibits an emergent critical charge fluctuation mode associated with Kondo breakdown, and secondly the 1D ferromagnetic ground-state is intrinsically quantum critical, transforming into a Fermi liquid with character-

istic scale of order the Zeeman coupling, upon application of a magnetic field. This last feature is strongly reminiscent of the observed physics of β -YbAlB₄, a point we return to later.

Our large N approach is obtained by casting the local moments as Schwinger bosons $S(j)_{\alpha\beta} = b_{j\alpha}^\dagger b_{j\beta}$, where $2S = n_b(j)$ is the number of bosons per site, each individually coupled to a K channel conduction sea, with Hamiltonian

$$H = \sum_j [H_{FM}(j) + H_K(j) + H_C(j) + \lambda_j(n_b(j) - 2S)], \quad (3)$$

where

$$\begin{aligned} H_{FM}(j) &= -(J_H/N)(b_{j\alpha}^\dagger b_{j+1,\alpha})(b_{j+1,\beta}^\dagger b_{j\beta}) \\ H_K(j) &= -(J_K/N)(b_{j\alpha}^\dagger \psi_{ja\alpha})(\psi_{ja\beta}^\dagger b_{j\beta}) \\ H_C(j) &= \sum_{\mathbf{p}} \epsilon_{\mathbf{p}} c_{\mathbf{p}\alpha}^\dagger(j) c_{\mathbf{p}\alpha}(j), \end{aligned} \quad (4)$$

where λ_j is a Lagrange multiplier that imposes the constraint. Here we have adopted a summation convention, with implicit summations over the (greek) $\alpha \in [1, N]$ spin and (roman) $a \in [1, K]$ channel indices. In the calculations, we take $2S = K = sN$ for perfect screening, where s is kept fixed and we have scaled the coupling constants that each term scales extensively with N .

Next, we factorize the interactions using Hubbard-Stratonovich transformations:

$$\begin{aligned} H_K(j) &\rightarrow [(b_{j\alpha}^\dagger \psi_{ja\alpha}) \chi_{ja} + \text{h.c.}] + \frac{N \bar{\chi}_{ja} \chi_{ja}}{J_K} \\ H_{FM}(j) &\rightarrow [\bar{\Delta}_j (b_{j+1,\alpha}^\dagger b_{j,\alpha}) + \text{h.c.}] + \frac{N |\Delta_j|^2}{J_H}. \end{aligned} \quad (5)$$

The first line is the Parcollet-Georges factorization of the Kondo interaction, where the χ_{ja} are charged, spinless Grassman fields that mediate the Kondo effect in channel a . The second line is the Arovas-Auerbach factorization of the magnetic interaction in terms of the bond variables Δ_j which describe the delocalization of the spinons. The b and χ fields both have non-trivial dynamics. The action admits a dynamical [26–29], saddle-point solution in the large- N limit, with self-energies given by [34]

$$\Sigma_\chi(\tau) = g_0(-\tau) G_B(\tau), \quad \Sigma_B(\tau) = -k g_0(\tau) G_\chi(\tau). \quad (6)$$

Here $G_\chi(\tau)$, $G_B(\tau)$ and $g(\tau)$ are the local propagators of the holons, spinons and conduction electrons, respectively. The conduction electron self-energy is of order $O(1/N)$ and can be neglected in the large- N limit, so that $g_0(\tau)$ is the bare local conduction electron propagator. The holon Green's function is purely local, given by $G_\chi(z) = [-J^{-1} - \Sigma_\chi(z)]^{-1}$, but the interesting new feature of our calculation is the delocalization of the spinons along the chain. Seeking uniform solutions where $\Delta_j = -\Delta$ and $\lambda_j = \lambda$, the spinons develop a dispersion $\epsilon_B(p) = -2\Delta \cos p$, with propagator $G_B(p, z) = [z - \epsilon_B(p) - \lambda - \Sigma_B(z)]^{-1}$. The momentum-summed local propagator is then

$$G_B(z) = \sum_p G_B(p, z) = \int \frac{d\epsilon_B \rho(\epsilon_B)}{z - \lambda - \epsilon_B - \Sigma_B(z)} \quad (7)$$

where

$$\rho(\epsilon_B) = \sum_p \delta[\epsilon - \epsilon_B(p)] = \frac{(2\pi\Delta)^{-1}}{\sqrt{1 - (\epsilon_B/2\Delta)^2}}. \quad (8)$$

is the bare spinon density of states. Using Cauchy's theorem,

$$G_B(z) = \frac{1}{\Omega[z]} \frac{1}{\sqrt{1 - [\Omega(z)/2\Delta]^2}} \quad (9)$$

where $\Omega(z) \equiv z - \lambda - \Sigma_B(z)$ [34].

Stationarity of the Free energy with respect to λ and Δ then leads to two saddle-point equations

$$\int_{-\infty}^{+\infty} \frac{d\omega}{\pi} n_B(\omega) \text{Im}[G_B(\omega - i\eta)] = s, \quad (10)$$

$$\frac{1 + \zeta \frac{\Delta^2}{J_H^2}}{J_H} = \int \frac{d\omega}{2\pi\Delta^2} n_B(\omega) \text{Im}[\Omega(z)G_B(z)]_{z=\omega+i\eta} \quad (11)$$

which determine λ and J_H self-consistently.

In equation (11) we have added an additional $\zeta \frac{\Delta^2}{J_H^2}$ which stabilizes the quantum critical point. Schwinger boson mean-field theories suffer from weak first order phase transitions upon development of finite Δ , which can be traced back to fluctuation-induced attractive quartic $O(\Delta^4)$ terms in the effective action. This difficulty [35], has thwarted the study of quantum criticality with this method. In our work, we have shown that these first order transitions are actually a non-universal artifact of the way the large N limit is taken, easily circumvented by adding a small repulsive biquadratic term $H'(j) = \zeta J_H (\vec{S}_j \cdot \vec{S}_{j+1})^2$ to the Hamiltonian. For an $SU(2)$ $S = 1/2$ moment, the biquadratic term can be absorbed into the Heisenberg interaction, but for the higher spin representations of the large N expansion, it contributes a positive quartic correction $O(\zeta\Delta^4)$ to the effective action that restores the second-order phase transitions (at both zero and finite temperature) to the large N limit [34]. In practice, a $\zeta \sim 0.001$ is sufficient to remove the first order transition, so that Δ tunes linearly with J_H across the quantum critical point.

To find $G_B(\omega)$ and $G_\chi(\omega)$ we solve Eqs. (6-10) self-consistently on a linear and logarithmic grid. The entropy formula from [28, 29] was used to compute the specific heat associated with these solutions [34].

We now describe our results in detail. In the Kondo limit ($x = T_K/J_H \gg 1$) the local moments are fully screened, forming a Fermi liquid; in the Schwinger boson scheme, the formation of Kondo-singlets is manifested as a spectral gap $\Delta_g \sim T_K$ [29] in the spectrum of the spinons and holons, where $T_K = f(T_K^0, s)$ and $T_K^0 = De^{-1/\rho J}$ is the Kondo temperature. The opening of this gap effectively confines the spinon and conduction electron into a singlet bound state, leaving behind an elastic resonant scattering potential which satisfies the Friedel sum rule with phase shift $\delta = \pi/N$.

In the opposite ferromagnetic limit $x = T_K/J_H \ll 1$, the chain forms a fragile ferromagnet. In this case, the spinons

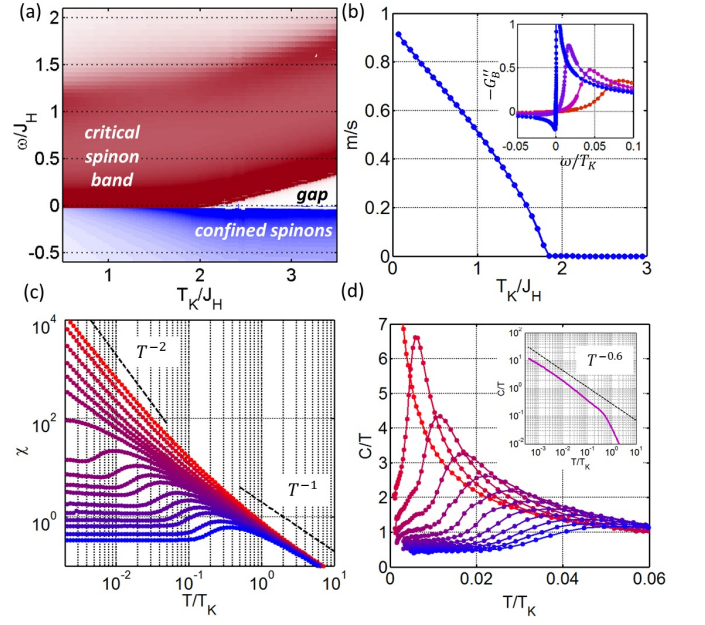


FIG. 2. (a) The spectral function of spinon boson $-G''_B(\omega + i\eta)$ for $k = s = 0.3$ as a function of $x = T_K/J_H$. The spinon band at positive energy and the Kondo-screened spins appearing as confined spinons at negative energy are marked. The Kondo gap at large x , shrinks linearly with lowering x , collapsing at about $x \approx 2$. (b) Top: The zero temperature magnetization m/s as a function of T_K/J_H . Inset: the evolution of the spectral function with temperature. (c) uniform spin susceptibility and (b) specific heat coefficient $\gamma(T) = C/T$ vs. temperature as T_K/J_H is varied from 5 (blue) to 0.1 (red). The inset in (d) shows the power law dependence of γ at the QCP.

are condensed in the ground-state, but at finite temperatures, the spinon band is gapped: the constraint (10) ensures that the gap in the spectrum grows quadratically, $\Delta_b(T) \propto T^2$, and together with the quadratic dispersion, this leads to a free energy $F \propto T^{3/2}$, a critical susceptibility $\chi \propto T^{-2}$ and a specific heat coefficient $C/T \propto T^{-1/2}$ [25, 34], in agreement with Bethe ansatz [36–39]. The van-Hove singularity of density of states (8) means that the ferromagnet is fragile, so that the bosons only condense, developing true long-range order at absolute zero temperature.

Fig. 2 shows the evolution of properties between these two limits. As x is reduced, the spectral gap responsible for Fermi liquid behavior shrinks linearly with x , collapsing to zero at the QCP at $x_c \approx 2$. This collapse is an indication of Kondo break-down. This suppression of the Kondo temperature with x is closely analogous to reduction of a Kondo temperature by Hund's coupling [30, 33, 40], with $\Delta \sim J_H$ playing the role of the Hund's coupling and the ratio ξ/a of the spin correlation length to the lattice spacing, playing the role of the effective moment.

The ferromagnetic moment which develops in the ground-state is

$$m = \lim_{T \rightarrow 0} \int_0^\infty \frac{d\omega}{\pi} n_B(\omega) \text{Im} G_B(\omega - i\eta). \quad (12)$$

This is a measure of the ground-state magnetization because the spinon population left at positive energies, condenses at $T = 0$. The top panel in Fig. 2(b) shows m for various $x = T_K/J_H$. m is zero in the fully screened state, and rises gradually to a maximum value $m = s = 2S/N$ in the ferromagnetic limit. The zero-temperature magnetization grows continuously in the magnetic phase, indicating a second order quantum phase transition. Note that $m/s < 1$ indicates that the magnetic moment is partially screened by an incipient Kondo effect which continues into the fragile magnetic phase.

Fig. 2(c) shows the dependence of the uniform spin susceptibility on $x = T_K/J_H$. In the Fermi liquid at large x (blue), there is a cross over from a Curie susceptibility $\chi \sim 1/T$ at high- T to a Pauli susceptibility $\chi \sim 1/T_F$ at the Fermi temperature T_F . As x decreases, T_F decreases to zero and the susceptibility becomes critical. At the QCP in the large N , the susceptibility $\chi \sim 1/T$ follows a simple Curie law. For $x < x_c$, the susceptibility displays a $\chi \sim 1/T^2$ characteristic of 1D FM. Similarly, the specific heat coefficient $\gamma \equiv C/T = dS/dT$, shown in Fig. 2(d) shows a ‘‘Schottky’’ peak at $T \sim T_F$ for large x (blue) which moves to zero as x is reduced (red). At the QCP, $\gamma(T) \sim T^{-\alpha}$ follows a power-law, where $\alpha[s]$ depends on the reduced spin $s = 2S/N$. In the calculations displayed here, $\alpha = 0.6$ for $s = 0.3$ (Fig. 2 d). In the magnetic phase $\gamma \sim 1/\sqrt{T}$ again characteristic of 1D FM.

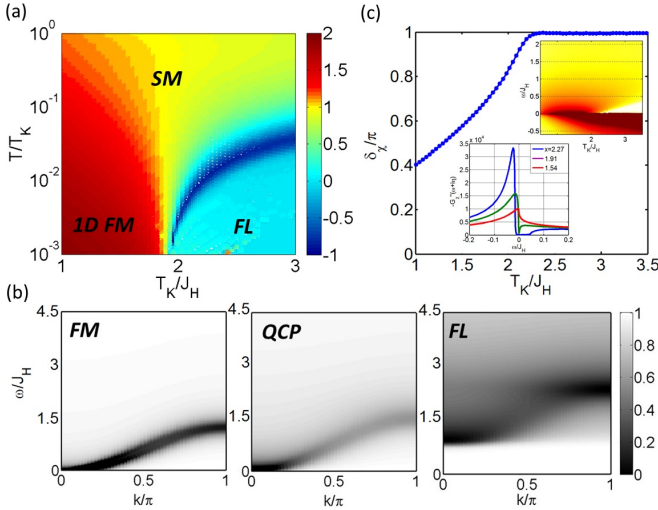


FIG. 3. (a) The static spin susceptibility exponent shows the Kondo breakdown induced by the Schrieffer suppression of the Fermi temperature and separated from the magnetic phase by a QCP. (b) The phase shift of holons $\delta\chi/\pi$ vs. T_K/J_H at $T/T_K = 0.01$. Top inset: The spectral density of holons $-G''_\chi(\omega + i\eta)$ as a function of T_K/J_H shows the Kondo-gap collapse and the critical mode near QCP. Bottom inset: The spectral density of holons in FL (blue), QCP (green) and FM (red) phases. (c) Dynamical spin susceptibility in FL ($T_K/J_H = 3.6$), QCP (1.65) and FM (0.36) regimes, respectively.

Fig. 3 shows the evolution of the magnetic susceptibility across the phase diagram. Fig. 3(a) displays the dependence of the temperature exponent $-d \log \chi / d \log T$ of the susceptibil-

ity on x and temperature. The dark blue stripe delineates the renormalized Fermi temperature of the Fermi liquid, showing its collapse to zero as $x \rightarrow x_c^+$. The corresponding evolution in the dynamical magnetic susceptibility $\chi''(q, \omega)$ of various phases are shown in Fig. 3(b). The sharp magnon band in the magnetic phase is smeared at the QCP, denoting fractionalization of the spins. The FL phase features a spectral gap as well as some remnants of the magnon band.

Although our simple model does not allow us to examine the evolution of the Fermi surface, we can monitor the delocalization of heavy electrons by examining the phase shift of the holons $\delta\chi = \text{Im} \ln[-G_\chi^{-1}(0 - i\delta)]$. The holons represent the Kondo singlets formed between spinons and conduction holes, and they behave as a spinless, positively charged background that compensates the delocalized heavy electrons. The change in the number of delocalized heavy electrons Δn_f is related to the holon phase shift by the relation $\Delta n_f = \sum_a (\frac{\delta\chi_a}{\pi})$ [28, 29], so we can monitor the change in the number of delocalized heavy fermions by looking at the holon phase shift. In the FL phase, the holons form a fully occupied band of fermions with $\delta\chi = \pi$, protected by the energy gap T_K . Fig. 3(c) shows the holon phase shift at low temperatures as a function of x . Interestingly, even in the magnetic phase and close to the QCP the holon phase shift remains finite, and there are still bound holons beneath the Fermi energy, indicating the persistence of the Kondo effect into the magnetic phase. Although we do not observe a jump in $\delta\chi$ at the QCP, there is a sharp cusp in its evolution at $x = x_c$. One of the unexpected aspects of our results, is that the holon spectrum becomes critical at the QCP, signaling the emergence of a critical spinless charge fluctuation that accompanies the critical formation and destruction of singlets (insets of Fig. 3(c)).

We have also studied the effect of applying a magnetic field [34]. The Fermi liquid is robust against a magnetic field, and a field produces small quadratic shifts in the various mean-field quantities. However, in the gapless phases, application of a small magnetic field [41, 42] has a profound effect: it reinstates Fermi-liquid behavior with a scale T_B set by the Zeeman energy (at the QCP) or a combination of the spinon bandwidth and magnetic field (in the FM phase). This is shown in Figs. 4(a,b) for susceptibility χ and the specific heat coefficient γ . In this sense, both the quantum critical point and the ferromagnetic phase are intrinsically quantum critical.

To conclude, we have studied a microscopic model of quasi-1D Kondo lattice with ferromagnetic coupling between the spins. By mapping the Ising limit of the model to the transverse field Ising model we have been able to establish the existence of a ferromagnetic quantum critical point. By using a dynamical large- N technique we have studied Heisenberg limit and aspects of the problem that go beyond Ising criticality, we have identified a Fermi liquid and a critical 1D FM phase, separated by a QCP governed by continuous drop in the Kondo temperature. Moreover, holon phase shift suggests the presence of a new fermionic mode of charge fluctuations at the QCP, which is caused by the critical and dynamical formation

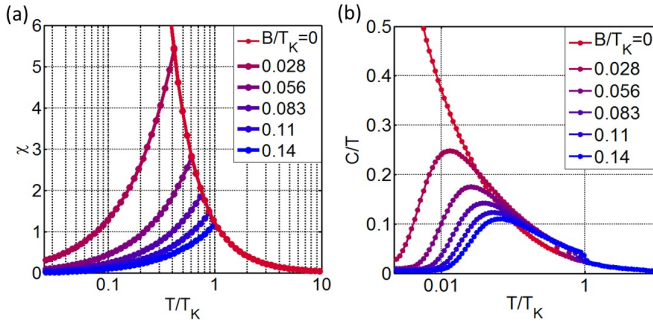


FIG. 4. Application of a magnetic field at $T_K/J_H = 0.1$ drives the (a) susceptibility χ and (b) specific heat coefficient γ from the critical behavior (red) to a FL behavior (blue). The kinks are due to the finite temperature BEC transition in the spinons in presence of the magnetic field.

and annihilation of Kondo singlets. In the 1D FM phase, the Kondo coupling $J \sim -G'_\chi(0 + i\eta)$ remains finite at low temperature, indicating a marginal coupling. Consequently, in addition to magnons, there exist short-lived holons (quasi-bound states of electrons and spinons) with the density $1 - m/s$, implying a two-fluid picture [43].

A natural extension to our work is to study the case of anti-ferromagnetic coupling. A more computationally involved extension would be to allow electrons to hop between the wires, which create momentum dependence for the Green's functions. Generalizations to higher dimensional systems can be envisioned by using our quasi-1D system as an extended impurity for the dynamical mean-field theory (DMFT) [44].

There are two interesting questions arising from our work. First, the intrinsic quantum criticality of the 1D FM phase is reminiscent of β -YbAlB₄ with many similar aspects to the thermodynamics and sensitivity to magnetic field. Yet our model is a very over-simplified 1D model. This raises the fascinating question as to whether the critical 1D FM seen in our model might be stabilized as a phase in higher dimensions, perhaps through antiferromagnetic frustration within the honey-comb lattice that connects the Yb chains in β -YbAlB₄? Here, the partial Kondo screening of the Yb ions might act to increase the magnetic fluctuations driving a kind of spin-liquid transition between the chains. We also note that a similar material, YbNi₄P₂ has a finite Curie temperature at ambient pressure and that it is only by applying a chemical pressure that the transition is shifted to zero temperature.

The second issue concerns the character of the Kondo break-down at the QCP. The break-down of Kondo screening at the QCP appears to involve an emergent singlet charge degree of freedom, which in our theory is a critical spinless mode. It is fascinating to speculate whether this might be an essential element of a future theory of heavy fermion quantum criticality.

ACKNOWLEDGEMENT

This work was supported by a Rutgers University Materials Theory postdoctoral fellowship (YK), and by NSF grant DMR-1309929 (PC). YK acknowledges discussions with E. König, T. Ayrar and P. Schlottmann.

- [1] F. Steglich and S. Wirth, *Reports on progress in physics. Physical Society (Great Britain)* **79**, 084502 (2016).
- [2] P. Coleman, *Introduction to Many-Body Physics* (Cambridge University Press, 2015).
- [3] J. A. Hertz, *Phys. Rev. B* **14**, 1165 (1976).
- [4] A. J. Millis, *Phys. Rev. B* **48**, 7183 (1993).
- [5] T. Moriya and T. Takimoto, *Journal of the Physical Society of Japan* **64**, 960 (1995).
- [6] Q. Si, S. Rabello, K. Ingersent, and J. L. Smith, *Nature* **413**, 804 (2001).
- [7] T. Senthil, S. Sachdev, and M. Vojta, *Phys. Rev. Lett.* **90**, 216403 (2003).
- [8] P. Coleman and A. H. Nevidomskyy, *Journal of Low Temperature Physics* **161**, 182 (2010).
- [9] Q. Si and F. Steglich, *Science* **329**, 1161 (2010).
- [10] S. Doniach, *Physica B+C* **91**, 231 (1977).
- [11] A. Schroder, G. Aeppli, R. Coldea, M. Adams, O. Stockert, H. Lohneysen, E. Bucher, R. Ramazashvili, and P. Coleman, *Nature* **407**, 351 (2000).
- [12] H. v. Löhneysen, A. Rosch, M. Vojta, and P. Wölfle, *Rev. Mod. Phys.* **79**, 1015 (2007).
- [13] Y. Nakatsuji, K. Kuga, Y. Machida, T. Tayama, T. Sakakibara, Y. Karaki, H. Ishimoto, S. Yonezawa, Y. Maeno, E. Pearson, G. G. Lonzarich, L. Balicas, H. Lee, and Z. Fisk, *Nat Phys* **4**, 603 (2008).
- [14] Y. Matsumoto, S. Nakatsuji, K. Kuga, Y. Karaki, N. Horie, Y. Shimura, T. Sakakibara, A. H. Nevidomskyy, and P. Coleman, *Science* **331**, 316 (2011).
- [15] Y. Matsumoto, S. Nakatsuji, K. Kuga, Y. Karaki, Y. Shimura, T. Sakakibara, A. H. Nevidomskyy, and P. Coleman, *Journal of Physics: Conference Series* **391**, 012041 (2012).
- [16] A. Steppke, R. Küchler, S. Lausberg, E. Lengyel, L. Steinke, R. Borth, T. Lühmann, C. Krellner, M. Nicklas, C. Geibel, F. Steglich, and M. Brando, *Science* **339**, 933 (2013).
- [17] R. E. Baumbach, H. Chudo, H. Yasuoka, F. Ronning, E. D. Bauer, and J. D. Thompson, *Phys. Rev. B* **85**, 094422 (2012).
- [18] R. Miyazaki, Y. Aoki, R. Higashinaka, H. Sato, T. Yamashita, and S. Ohara, *Phys. Rev. B* **86**, 155106 (2012).
- [19] S. J. Yamamoto and Q. Si, *Proceedings of the National Academy of Sciences* **107**, 15704 (2010).
- [20] A. H. Nevidomskyy and P. Coleman, *Phys. Rev. Lett.* **102**, 077202 (2009).
- [21] G. Toulouse, *Comptes Rendu Academie Science* **268**, 1200 (1969).
- [22] V. J. Emery and S. Kivelson, *Phys. Rev. B* **46**, 10812 (1992).
- [23] Y. Komijani and P. Coleman, in preparation (2017).
- [24] S. Sachdev, *Quantum Phase Transitions*, 2nd ed. (Cambridge University Press, 2011).
- [25] D. P. Arovas and A. Auerbach, *Phys. Rev. B* **38**, 316 (1988).
- [26] O. Parcollet and A. Georges, *Phys. Rev. Lett.* **79**, 4665 (1997).
- [27] O. Parcollet, A. Georges, G. Kotliar, and A. Sengupta, *Phys. Rev. B* **58**, 3794 (1998).

- [28] P. Coleman, I. Paul, and J. Rech, *Phys. Rev. B* **72**, 094430 (2005).
- [29] J. Rech, P. Coleman, G. Zarand, and O. Parcollet, *Phys. Rev. Lett.* **96**, 016601 (2006).
- [30] J. R. Schrieffer, *Journal of Applied Physics* **38**, 1143 (1967).
- [31] A. I. Larkin and V. I. Mel'nikov, *Soviet Physics JETP* **34**, 656 (1972).
- [32] K. Haule and G. Kotliar, *New Journal of Physics* **11**, 025021 (2009).
- [33] A. H. Nevidomskyy and P. Coleman, *Phys. Rev. Lett.* **103**, 147205 (2009).
- [34] See supplementary material.
- [35] T. N. De Silva, M. Ma, and F. C. Zhang, *Phys. Rev. B* **66**, 104417 (2002).
- [36] P. Schlottmann, *Phys. Rev. Lett.* **54**, 2131 (1985).
- [37] P. Schlottmann, *Phys. Rev. B* **33**, 4880 (1986).
- [38] M. Takahashi and M. Yamada, *Journal of the Physical Society of Japan* **54**, 2808 (1985).
- [39] M. Takahashi, *Phys. Rev. Lett.* **58**, 168 (1987).
- [40] I. Okada and K. Yosida, *Progress of Theoretical Physics* **49**, 1483 (1973).
- [41] P. Coleman and C. Pépin, *Phys. Rev. B* **68**, 220405 (2003).
- [42] P. Coleman and I. Paul, *Phys. Rev. B* **71**, 035111 (2005).
- [43] P. Monthoux and D. Pines, *Phys. Rev. B* **47**, 6069 (1993).
- [44] A. Georges, G. Kotliar, W. Krauth, and M. J. Rozenberg, *Rev. Mod. Phys.* **68**, 13 (1996).

SUPPLEMENTARY MATERIAL

Ferromagnetically coupled spin chain

Here, we briefly review the Arovas and Auerbach [25] treatment of 1D ferromagnetism. In absence of Kondo coupling, the Hamiltonian is $H_\lambda + H_{FM}$ where H_λ refers to the Lagrange multipliers. We assume a uniform mean-field solution Δ and find the temperature-dependence of the chemical potential.

Chemical potential - The number of bosons satisfies

$$s = \int_{-\pi}^{\pi} \frac{dk}{2\pi} n_B(\lambda + \epsilon_k) = \int d\epsilon \rho(\epsilon) n_B(\epsilon + \lambda), \quad (13)$$

When $T \ll \Delta$, the Bose Einstein function n_B is highly focused at low energies, and the physics is dominated by the quadratic bottom of the spinon band where $\epsilon_k = -2\Delta \cos k \approx -2\Delta + \Delta k^2$ so that

$$\rho(\epsilon) = \frac{2}{2\pi d\epsilon_k/dk} = \frac{1}{2\pi\Delta \sin k} \sim \frac{1}{2\pi\sqrt{\Delta}\sqrt{\epsilon + 2\Delta}}. \quad (14)$$

The factor of 2 in the numerator derives from the 2-to-1 relation between the momentum and energy ϵ_k . Using $\epsilon' = \epsilon + 2\Delta$ and $\lambda' = \lambda - 2\Delta$, we can write

$$\begin{aligned} s &= \frac{1}{2\pi\sqrt{\Delta}} \int_0^\infty d\epsilon' \frac{1}{\sqrt{\epsilon'}} \frac{1}{e^{\beta(\lambda' + \epsilon')} - 1} \\ &= \frac{1}{2\pi} \sqrt{\frac{T}{\Delta}} \Gamma(1/2) \text{Li}_{1/2}(z), \end{aligned} \quad (15)$$

where we have defined the fugacity $z \equiv e^{-\beta\lambda'}$ and used that

$$\begin{aligned} I_p(z) &\equiv \int_0^\infty dx \frac{x^{p-1}}{e^x/z - 1} \\ &= \sum_{k=0}^\infty \frac{z^{k+1}}{(k+1)^p} \int_0^\infty dy y^{p-1} e^{-y} \\ &= \Gamma(p) \text{Li}_p(z), \end{aligned} \quad (16)$$

in terms of polylogarithm function $\text{Li}_p(z)$. For $z = 1$ and $p > 1$ the series is convergent and $\text{Li}_p(z) = \zeta(p)$ where $\zeta(p)$ is the Riemann zeta function. But for $p < 1$ we also get convergence if $|z| < 1$. Due to the \sqrt{T} prefactor in the expression for s in Eq. (15), the function $\text{Li}_{1/2}(z)$ has to diverge as $T \rightarrow 0$ so that s stays constant and this happens for $z \rightarrow 1$ for which we have

$$\lim_{z \rightarrow 1} \text{Li}_{1/2}(z) = \frac{\sqrt{\pi}}{\sqrt{-\log(z)}} = \frac{\sqrt{\pi}}{\sqrt{\lambda'/T}}. \quad (17)$$

Therefore, we conclude

$$\lambda' = \alpha T^2, \quad \alpha = \frac{\Gamma^2(1/2)}{2\pi\Delta s^2}. \quad (18)$$

Δ vs. J_H - This can also be alternatively written as

$$\frac{\Delta}{J_H} = -\frac{1}{2\Delta} \int d\epsilon \epsilon \rho(\epsilon) n_B(\lambda + \epsilon) \quad (19)$$

Again assuming that the bottom of the band is only involved (this works in the limit of large Δ/T) we have

$$2\frac{\Delta^2}{J_H} = -\frac{1}{2\pi\sqrt{\Delta}} \int_0^\infty d\epsilon' \frac{\epsilon' - 2\Delta}{\sqrt{\epsilon'}} \frac{1}{e^{\beta(\epsilon' + \lambda')} - 1} \quad (20)$$

$$= -\frac{1}{2\pi\sqrt{\Delta}} \left[T\sqrt{T} I_{3/2}(z) - 2\Delta\sqrt{T} I_{1/2}(z) \right], \quad (21)$$

in terms of $I_p(z)$ defined in Eq. (16). Equivalently

$$\frac{2\Delta^{5/2}}{J_H} = -\frac{1}{2\pi} \left[T\sqrt{T}\Gamma(3/2)\text{Li}_{3/2}(z) - 2\sqrt{T}\Delta\Gamma(1/2)\text{Li}_{1/2}(z) \right]. \quad (22)$$

So, using $z\partial_z \text{Li}_p(z) = \text{Li}_{p-1}(z)$ we find

$$2\frac{\Delta^{5/2}}{J_H} = \frac{1}{2\pi} \left[2\Gamma(1/2) \times \sqrt{\pi} \frac{\Delta}{\sqrt{\alpha\Delta}} + T^2 \sqrt{\alpha\Delta} 2\sqrt{\pi}\Gamma(3/2) \right]. \quad (23)$$

At zero temperature, we can drop the second term in the right side and from $\alpha_\Delta \propto s^2/\Delta$ find

$$2\frac{\Delta^{5/2}}{J_H} = 2s\Delta^{3/2} \rightarrow \Delta(T \rightarrow 0) = J_H s. \quad (24)$$

Susceptibility - The susceptibility is

$$\begin{aligned} \chi &= -\frac{dM}{dB} \Big|_{B=0} = \frac{\beta}{L} \sum_k n_B(\lambda + \epsilon_k) [1 + n_B(\lambda + \epsilon_k)] \\ &= -\frac{1}{L} \sum_k \frac{-\beta e^{\beta(\lambda + \epsilon_k)}}{(e^{\beta(\lambda + \epsilon_k)} - 1)^2} \end{aligned} \quad (25)$$

Doing the momentum sum we find

$$\begin{aligned} \chi &= \beta \int \frac{dk}{2\pi} \frac{e^{\beta(\lambda + \epsilon_k)}}{[e^{\beta(\lambda + \epsilon_k)} - 1]^2} \\ &= \beta \int_0^\infty d\epsilon' \rho(\epsilon' - 2\Delta) \frac{e^{T\epsilon'/z}}{[e^{T\epsilon'/z} - 1]^2} \\ &= \frac{\beta}{4\pi\sqrt{\Delta}} \sqrt{T} \int_0^\infty dx \frac{1}{\sqrt{x}} \left\{ \frac{e^x/z}{[e^x/z - 1]^2} \right\} \\ &= \frac{T^{-1/2}}{4\pi\sqrt{\Delta}} \Gamma(1/2) \text{Li}_{-1/2}(z) \\ &\rightarrow \frac{\alpha^{-3/2}}{8\sqrt{\pi}\sqrt{\Delta}} \frac{1}{T^2}. \end{aligned} \quad (26)$$

where the last line is valid in the limit of low-temperature.

Free energy - This is simply

$$\begin{aligned} F + \lambda s &= \int \frac{d\omega}{\pi} n_B(\omega) \int d\epsilon \rho(\epsilon) \text{Im} [\log(\epsilon + \lambda - \omega - i\eta)] \\ &= \int \frac{d\omega}{\pi} \frac{n_B(\omega)}{2\pi\sqrt{\Delta}} \int_0^\infty \frac{d\epsilon'}{\sqrt{\epsilon'}} \text{Im} [\log(\epsilon' + \lambda' - \omega - i\eta)] \\ &= -\pi \frac{1}{2\pi\sqrt{\Delta}} \int \frac{d\omega}{\pi} n_B(\omega) \int_0^{\omega - \lambda'} \frac{d\tilde{\epsilon}}{\sqrt{\tilde{\epsilon}}} \\ &= -\pi \frac{1}{\pi\sqrt{\Delta}} \int \frac{d\omega}{\pi} n_B(\omega) \sqrt{\omega - \lambda'}. \end{aligned} \quad (27)$$

After a $\omega = \lambda' + Tx$ change of variable,

$$\begin{aligned} F &= -\lambda s - \frac{1}{\pi\Delta} T^{3/2} \int_0^\infty \frac{dx\sqrt{x}}{e^{x/z} - 1} \\ &= -2\Delta s - \lambda' s - \frac{T^{3/2}}{\pi\Delta} \Gamma(3/2) \text{Li}_{3/2}(z) \end{aligned} \quad (28)$$

The polylogarithm has the expansion

$$\text{Li}_{3/2}(z) = -2\sqrt{\pi \log(-z)} + \sum_{m=0} \frac{\log^m(z) \zeta(1/2 - m)}{m!}.$$

Inserting this and also Eq. (18) into Eq. (28),

$$\begin{aligned} F &= -2\Delta s - \frac{T^2 \Gamma(1/2)}{2\pi\Delta s} [\Gamma(1/2) - 2\Gamma(3/2)] \\ &\quad - \frac{T^{3/2}}{\pi\sqrt{\Delta}} \Gamma(3/2) \zeta(1/2) + \dots \end{aligned} \quad (29)$$

Remarkably, the T^2 term is cancelled out due to $\partial_\lambda F = 0$ and the second line contributes a $F_T - F_0 \propto T^{3/2}$, giving a $S = -dF/dT \sim \sqrt{T}$ entropy and a $\gamma = C/T \propto 1/\sqrt{T}$ specific heat coefficient.

Dynamical large- N equations

We start from the Hamiltonian (2) in the paper. The interaction part of the action is

$$S_I = \frac{1}{\sqrt{N}} \sum_{j\alpha\alpha'} \int_0^\beta d\tau [\chi_{ja}(\tau) \bar{b}_{j\alpha}(\tau) \psi_{ja\alpha}(\tau) + \text{h.c.}] \quad (30)$$

First we integrate out the c -electron. The result is

$$S_I = \frac{1}{N} \sum_{j\alpha\alpha'} \int_0^\beta d\tau_1 d\tau_2 \left[\chi_{ja}(\tau_1) b_{j\alpha}^\dagger(\tau_1) g_0(\tau_1 - \tau_2) b_{j\alpha}(\tau_2) \chi_{ja}^\dagger(\tau_2) \right] \quad (31)$$

where $g_0(\tau)$ is the bare local conduction electron propagator. We decouple this by adding to the action a conjugate pair of two-point quantum fields

$$S' = N \int_0^\beta d\tau_1 d\tau_2 \hat{G}_B(\tau_2, \tau_1) \hat{\Sigma}_B(\tau_1, \tau_2) \quad (32)$$

by shifting

$$\begin{aligned} \hat{G}_B(\tau_2, \tau_1) &\rightarrow \hat{G}_B(\tau_2, \tau_1) + \frac{1}{N} \sum_{j\alpha} b_{j\alpha}^\dagger(\tau_1) b_{j\alpha}(\tau_2) \\ \hat{\Sigma}_B(\tau_1, \tau_2) &\rightarrow \hat{\Sigma}_B(\tau_1, \tau_2) + \frac{1}{N} g_0(\tau_1, \tau_2) \sum_{ja} \chi_{ja}^\dagger(\tau_2) \chi_{ja}(\tau_1). \end{aligned}$$

we find

$$S' + S_I \rightarrow S' + \int_0^\beta d\tau_1 d\tau_2 \left[\sum_{n\alpha} b_{n\alpha}^\dagger(\tau_1) \hat{\Sigma}_B(\tau_1, \tau_2) b_{n\alpha}(\tau_2) + \sum_{nk} \chi_{nk}^\dagger(\tau_1) g_0(\tau_2, \tau_1) \hat{G}_B(\tau_1, \tau_2) \chi_{nk}(\tau_2) \right] \quad (33)$$

The free energy (the effective action times T) is

$$F[\hat{G}_B, \hat{\Sigma}_B] = NT \text{Tr} \log[\hat{\Sigma}_B(\tau_1, \tau_2) - G_{B0}^{-1}(\tau_1, \tau_2)] - N\lambda s - K T \text{Tr} \log[g_0(\tau_2, \tau_1) \hat{G}_B(\tau_1, \tau_2) - G_{\chi 0}^{-1}(\tau_1, \tau_2)] + NT \int_0^\beta d\tau_1 d\tau_2 \hat{G}_B(\tau_2, \tau_1) \hat{\Sigma}_B(\tau_1, \tau_2) \quad (34)$$

where

$$G_{B0}^{-1}(\tau_1, \tau_2) = -(\partial_{\tau_1} + \lambda) \delta(\tau_1 - \tau_2) \quad (35)$$

$$G_{\chi 0}^{-1}(\tau_1, \tau_2) = -J_K^{-1} \delta(\tau_1 - \tau_2). \quad (36)$$

Here variables \hat{O} with a hat on them, are fluctuating variables that are integrated over inside the path integral. In the limit of large- N , we can carry out a mean-field treatment of the path integral by replacing it by its saddle-point value. Variation of the free energy w.r.t. Σ_B gives $[\Sigma_B - G_{B0}^{-1}]^{-1} + G_B = 0$, so G_B and Σ_B obey a Dyson equation. Before we carry out the variation w.r.t. G_B , it is convenient to define $\Sigma_\chi(\tau_1, \tau_2) \equiv g_0(\tau_2, \tau_1) G_B(\tau_1, \tau_2)$. If we furthermore define $G_\chi(\tau_1, \tau_2) = [G_{\chi 0}^{-1} - \Sigma_\chi]^{-1}(\tau_1, \tau_2)$, then variation of the free energy w.r.t. G_B gives

$$\Sigma_B(\tau_1, \tau_2) = -\gamma g_0(\tau_2, \tau_1) G_\chi(\tau_1, \tau_2) \quad (37)$$

These set of self-consistent equations have a time-translationally invariant solution, dependent only on the time difference $\tau_1 - \tau_2$.

We now show that these mean-field equations can be obtained as the saddle point of a Kadanoff-Baym free energy functional. By identifying the argument of first logarithm in (34) as G_B^{-1} , we rewrite the free energy as

$$(NL)^{-1} F[G_B] = T \text{Tr} \left\{ \log[-G_B^{-1}] + (G_{B0}^{-1} - G_B^{-1}) G_B \right\} - \lambda s + f_3[G_B],$$

$$f_3[G_B] = -\gamma T \text{Tr} \log\{\Sigma_\chi[G_B] - G_{\chi 0}^{-1}\}$$

with $\Sigma_\chi[G_B] = g_0(\tau_2, \tau_1) G_B(\tau_1, \tau_2)$. If we take variations of this expression w.r.t. G_B , we recover expression (37). Next we elevate the free energy to a functional of G_χ and Σ_χ by rewriting f_3 as follows:

$$f_3[G_B] \rightarrow f_3[G_B, \Sigma_\chi, G_\chi]$$

$$= -\gamma T \text{Tr} \log[\Sigma_\chi - G_{\chi 0}^{-1}] - \gamma T \text{Tr} [\Sigma_\chi G_\chi] + \gamma T \text{Tr} [\Sigma_\chi[G_B] \times G_\chi].$$

Here, the last two terms basically cancel each other. If we set the variation of f_3 w.r.t. G_χ to zero, we recover $\Sigma_\chi = \Sigma_\chi[G_B]$. If we set the variation of f_3 w.r.t. Σ_χ to zero (only the

first two terms have to be taken into account) we find $G_\chi = [G_{\chi 0}^{-1} - \Sigma_\chi]^{-1}$ as we had above. Using the variation with respect to Σ_χ to get rid of Σ_χ in favor of G_χ , we find

$$f_3 = -\gamma T \text{Tr} \left\{ \log[-G_\chi^{-1}] + (G_{\chi 0}^{-1} - G_\chi^{-1}) G_\chi \right\} + \gamma T \text{Tr} [\Sigma_\chi[G_B] \times G_\chi] \quad (38)$$

and this gives us final expression for the free energy in the form of a Luttinger-Ward functional of Green's functions

$$(NL)^{-1} F[G] = T \text{Tr} \left[\log(-G_B^{-1}) + (G_{B0}^{-1} - G_B^{-1}) G_B \right] - \gamma T \text{Tr} \left[\log(-G_\chi^{-1}) - (G_{\chi 0}^{-1} - G_\chi^{-1}) G_\chi \right] + T \mathcal{Y}[G_\chi, G_B] - \lambda s, \quad (39)$$

where

$$\mathcal{Y}[G_\chi, G_B] = \gamma \text{Tr} [\Sigma_\chi[G_B] \times G_\chi] \quad (40)$$

$$= \gamma \beta \int_0^\beta d\tau g_0(\tau) G_B(-\tau) G_\chi(\tau) \equiv \beta Y$$

or in real frequency

$$Y = \gamma \int \frac{d\omega_1}{\pi} \int \frac{d\omega_2}{\pi} f(\omega_1) f(\omega_2) G_\chi''(\omega_1) \text{Im} [g_0(\omega_2) G_B(\omega_1 + \omega_2)] - \gamma \int \frac{d\omega_1}{\pi} \int \frac{d\omega_2}{\pi} n_B(\omega_1) f(\omega_2) G_B''(\omega_1) \text{Im} [g_0(\omega_2) G_\chi^*(\omega_2 - \omega_1)].$$

The diagrammatic rationale for the self-energies (6) is shown in Fig. (5). Note that since $\delta F[G]/\delta G = 0$, the self-energies can be obtained from the Luttinger-Ward functional $\Sigma = \delta Y/\delta G$. $\Sigma_B(\tau) = -\gamma g_0(\tau) G_\chi(\tau)$ gives in real-frequency

$$\Sigma_B(\omega + i\eta) = \gamma \int_{-\infty}^{+\infty} \frac{d\omega'}{\pi} f(\omega') \left\{ g_c''(\omega') G_\chi^R(\omega - \omega') - g_c^R(\omega + \omega') G_\chi''(-\omega') \right\}, \quad (41)$$

and $\Sigma_\chi(\tau) = g_0(-\tau) G_B(\tau)$ gives in real-frequency

$$\Sigma_\chi^R(\omega + i\eta) = \int_{-\infty}^{+\infty} \frac{d\omega'}{\pi} \left[-G_B^R(\omega + \omega') f(\omega') g_c''(\omega') + G_B''(\omega') n_B(\omega') g_c(\omega' - \omega - i\eta) \right]. \quad (42)$$

To find self-consistent solution to the dynamical large- N equations, we have implemented Eqs. (41) and (42) on a linear and logarithmic frequency grid, iteratively, together with the corresponding Dyson's equations. We start at high-temperature and gradually reduce the temperature to have convergence.

Fig. (6) summarizes some aspects of the single-impurity Kondo physics as captured by the large- N approach [26].

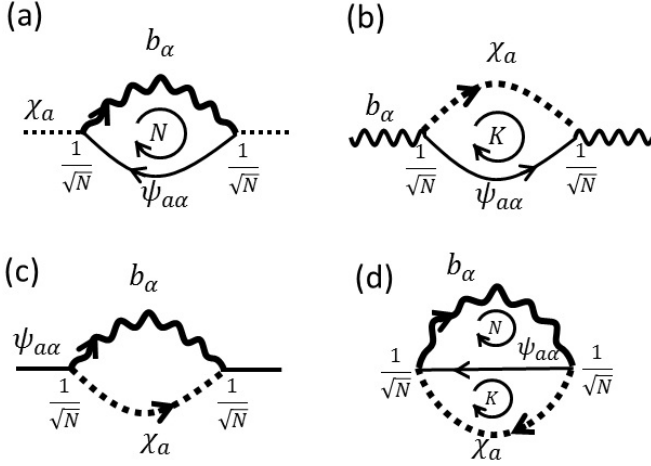


FIG. 5. (a-c) Diagrams for self-energy of (a) holon and (b) spinon and (c) the conduction electron. In two first two cases, the summation over the loop index (spin for holon and channel for boson) gives a factor of N which compensates $1/N$ coming from vertices, whereas no compensation in (c) means that conduction electron self-energy vanishes to $O(1)$ and corresponding Green's function remains bare. (d) The interaction part of the Luttinger-Ward functional. The self-energies can be obtained by cutting the corresponding propagator in this diagram $\Sigma = \delta Y / \delta G$.

Entropy

The free energy worked out in previous section is a stationary functional with respect to G_B , G_χ and λ . Keeping those constant, we take derivative w.r.t T to obtain the entropy. The result is [29]

$$S(T) = - \int \frac{d\omega}{\pi} \partial_T n_B(\omega) \left\{ \text{Im} \sum_k \log[-G_B^{-1}(k, \omega + i\eta)] + \Sigma_B''(\omega + i\eta) G_B'(\omega + i\eta) \right\} - k \int \frac{d\omega}{\pi} \partial_T f(\omega) \left\{ \text{Im} [\log[-G_\chi^{-1}(\omega + i\eta)]] + \Sigma_\chi''(\omega + i\eta) G_\chi'(\omega + i\eta) - g_0''(\omega + i\eta) \tilde{\Sigma}_c'(\omega + i\eta) \right\} \quad (43)$$

Here, g_0 is the bare Green's function of conduction band. And $\tilde{\Sigma}_c(\tau) = N \Sigma_c(\tau)$ where $\Sigma_c(\tau) = \frac{1}{N} G_B(\tau) G_\chi(-\tau)$ is the self-energy of the conduction electrons, which in the frequency domain is

$$\tilde{\Sigma}_c(\omega + i\eta) = \int \frac{d\nu}{\pi} \left[n_B(\omega) G_B''(\nu + i\eta) G_\chi(\nu - \omega - i\eta) - f(\nu) G_\chi''(\nu) G_B(\omega + \nu + i\eta) \right]. \quad (45)$$

At low temperature $\partial_T f(\omega) \propto \beta \omega \delta'(\omega)$ and as the fermionic functions do not diverge in the large- Δ limit, the residual entropy is dominated by the bosonic terms in the first two lines of Eq. (43).

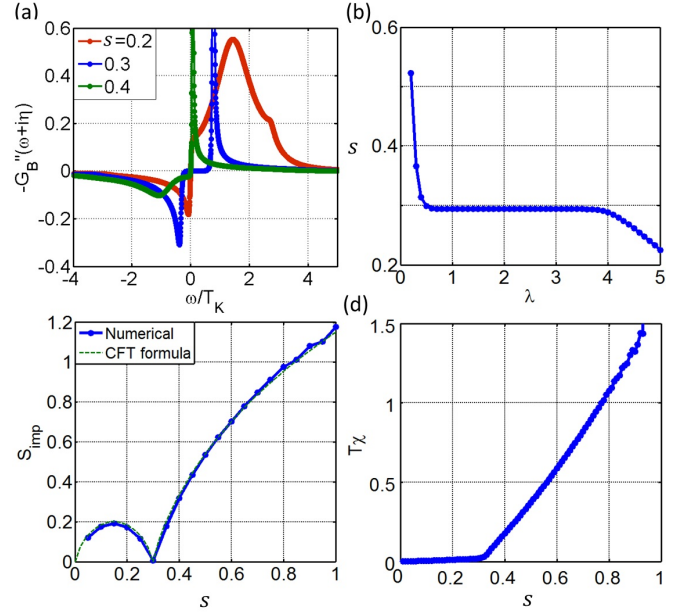


FIG. 6. The single-impurity Kondo physics from the large- N approach. $k = 0.3$ is fixed and s is varied. (a) The spectrum of spinons for fully-screened (blue) over-screened (red) and under-screened (green) cases. (b) The gap in λ vs. s for establishing a Fermi-liquid. (c) Residual entropy and (d) T_χ as a function of s , which captures the Curie susceptibility coming from the residual un-screened moments.

Momentum sums

In this section we sketch the derivation of Eq. (9) and the expression used for the calculation of the spin susceptibility.

According to Cauchy's theorem,

$$F(z) = \oint \frac{dz'}{2\pi i} \frac{F(z')}{z' - z} = \int \frac{d\omega}{\pi} \frac{1}{\omega - z} \text{Im} [F(\omega + i\eta)] \quad (46)$$

where the contour in the first integral is counter-clockwise and in the second expression we have assumed that the function $F(z')$ is analytical in the whole plane except on the real axis.

On the other hand for the local Green's function of the spinons we need to do the integral

$$G_B[\Omega(z)] = - \int \frac{d\epsilon_B \rho(\epsilon_B)}{\epsilon_B - \Omega(z)}, \quad \rho(\epsilon_B) = \frac{(2\pi\Delta)^{-1}}{\sqrt{1 - (\epsilon_B/2\Delta)^2}}.$$

where $\Omega(z) = z - \lambda - \Sigma_B(z)$. The function $\rho_B(\epsilon_B)$ can be expressed as the imaginary part of an analytical function

$$\rho(\epsilon_B) = -\text{Im} [F(\epsilon_B + i\eta)], \quad F(z) = \frac{1}{\pi z \sqrt{1 - (z/2\Delta)^{-2}}}.$$

Therefore, using (46), we find

$$G_B[\Omega(z)] = \frac{1}{\Omega \sqrt{1 - (\Omega/2\Delta)^{-2}}}. \quad (47)$$

The spin susceptibility can be expressed as the spinon bubble

$$\chi(k, \omega + i\eta) = \int \frac{dq}{2\pi} \int \frac{d\omega'}{\pi} n_B(\omega') G_B''(q, \omega') \quad (48)$$

$$[G_B(q + k, \omega' + \omega + i\eta) + G_B(q - k, \omega' - \omega - i\eta)].$$

For the static zero momentum case $k = \omega = 0$, we can write

$$\chi = \int \frac{d\omega}{\pi} n_B(\omega) \text{Im}[\chi_\omega], \quad \chi_\omega = \sum_k G_B^2(k, \omega + i\eta). \quad (49)$$

χ_ω can be expressed as the derivative of $G_B(z)$,

$$\chi_\omega = \int \frac{d\epsilon_B \rho(\epsilon_B)}{(\epsilon_B - \Omega)^2} = \frac{d}{d\Omega} G_B(\omega + i\eta). \quad (50)$$

Therefore, we find

$$\chi_\omega = -\frac{1}{2} \frac{\Omega}{[1 - (\Omega/2\Delta)^{-2}]}. \quad (51)$$

For the bosonic contribution to the entropy we need

$$\mathcal{S}_\omega = \sum_k \log[-G_B^{-1}(k, \omega + i\eta)] = \int d\epsilon_B \rho(\epsilon_B) \log[\epsilon_B - \Omega].$$

Similar to above, \mathcal{S}_ω can be expressed as $\mathcal{S}_\omega \sim \int d\Omega G_B$. So,

$$\mathcal{S}_\omega = \log \left[1 + \sqrt{1 - (\Omega/2\Delta)^{-2}} \right] + \log(\Omega/2)$$

assuming $\text{Re}[\Omega/2\Delta] \leq -1$.

Applying magnetic field

We assume that the B -field couples to all but one boson b_1 increasing their energy, so that the field-dependent “Zeeman” term in the Hamiltonian takes the form

$$H_Z = B \sum_{\alpha \neq 1} b_\alpha^\dagger b_\alpha$$

For an isolated spin, this means that one of the bosons has the energy λ whereas the others have the energy $\lambda + B$. There are two phases [41, 42]: a paramagnetic phase at high temperature in which the population of the low-energy boson is negligible $\langle b_1 \rangle = 0$ and λ is adjusted so that $n_B(\lambda + B) = s$. Lowering the temperature λ decreases until it becomes zero at $T/B = 1/\log[1 + 1/s]$ below which the low-energy boson undergoes a Bose-Einstein condensation (BEC) $\langle b_1 \rangle^2 = s - n_B(B)$ to accommodate an $O(N)$ magnetization, the polarized phase. In presence of Kondo screening and the spinon hopping, essentially similar arguments apply except that the spinon energies are dressed by the hopping and renormalized by the spin fluctuations. We start by writing the Hamiltonian

in a magnetic field (L is the system size)

$$H = N \sum_{ja} \frac{\chi_{ja}^\dagger \chi_{ja}}{J_K} + \sum_{ja\alpha} (\chi_{ja} b_{ja\alpha}^\dagger \psi_{ja\alpha} + \text{h.c.}) \quad (52)$$

$$+ \lambda \sum_j [\sum_\alpha b_{j\alpha}^\dagger b_{j\alpha} - 2S] + B \sum_{j,\alpha \neq 1} b_{j\alpha}^\dagger b_{j\alpha} + H_C$$

$$- \Delta \sum_{j\alpha} [b_{j\alpha}^\dagger b_{j+1,\alpha} + \text{h.c.}] + N \frac{\Delta^2}{J_H}. \quad (53)$$

Separating the low-energy boson from the rest we have

$$H = N \sum_{ja} \frac{\chi_{ja}^\dagger \chi_{ja}}{J_K} + \sum_{ja,\alpha \neq 1} (\chi_{ja} b_{ja\alpha}^\dagger \psi_{ja\alpha} + \text{h.c.})$$

$$+ N \frac{\Delta^2}{J_H} - \Delta \sum_{j,\alpha \neq 1} [b_{j\alpha}^\dagger b_{j+1,\alpha} + \text{h.c.}]$$

$$+ (\lambda + B) \sum_j [\sum_{\alpha \neq 1} b_{j\alpha}^\dagger b_{j\alpha} - 2S] + 2SB + H_C$$

$$+ (\lambda - 2\Delta) \sum_j b_{j,1}^\dagger b_{j,1} + \sum_{ja} (b_{j,1}^\dagger \chi_{ja} \psi_{ja,1} + \text{h.c.}). \quad (54)$$

We consider a mean-field solution in which the low-energy boson condenses $b_1 \rightarrow \langle b_1 \rangle$. The condition for BEC is that the energy of b_1 boson becomes zero. But the apparent energy $\lambda - 2\Delta$ is further renormalized by the charge fluctuations in the last term. After the condensation, the Hamiltonian is (by $\chi \rightarrow \tilde{\chi}/\sqrt{N}$)

$$H = \sum_j \frac{\tilde{\chi}_{ja}^\dagger \tilde{\chi}_{ja}}{J_K} + \frac{1}{\sqrt{N}} \sum_{ja,\alpha \neq 1} (\tilde{\chi}_{ja} b_{ja\alpha}^\dagger \psi_{ja\alpha} + \text{h.c.})$$

$$- \Delta \sum_{n,\alpha \neq 1} [b_{n\alpha}^\dagger b_{n+1,\alpha} + \text{h.c.}] + N \frac{\Delta^2}{J_H} + H_C$$

$$+ N(\lambda + B) \left[\frac{1}{N} \sum_{\alpha \neq 1} b_\alpha^\dagger b_\alpha - q \right] + NBq$$

$$+ NL(\lambda - 2\Delta) \langle b_1 \rangle'^2 + \langle b_1 \rangle' \sum_{ja} (\tilde{\chi}_{ja} \psi_{ja,1} + \text{h.c.}) \quad (55)$$

Since, $\langle b_1 \rangle$ is extensive, we have defined $\langle b_1 \rangle' = \langle b_1 \rangle / \sqrt{N}$. As long as the $\langle b_1 \rangle' = 0$, λ adjusts itself so that the spectrum does not move. Also, note that once b_1 condenses in a magnetic field, the value of Δ might change, but for small B this is negligible and we have discarded the B -dependence of the mean-field Δ in this paper. To find the condensate fraction, we minimize the energy with respect to $\langle b_1 \rangle'$. So we find

$$(\lambda - 2\Delta) \tilde{b}_1' = \frac{1}{NL} \sum_{ja} \text{Re} \langle \psi_{ja,1} \chi_{ja} \rangle \quad (56)$$

Considering that

$$\lim_{t \rightarrow 0} \langle \psi_{ja,1}(t) \chi_j(0) \rangle = i \int \frac{d\omega}{2\pi} G_{\psi\chi}^<(\omega), \quad (57)$$

and the relation

$$G_{\psi\chi}^<(\omega) = -f(\omega) [G_{\psi\chi}(\omega + i\eta) - G_{\psi\chi}(\omega - i\eta)], \quad (58)$$

we can write

$$(\lambda - 2\Delta)\bar{b}'_1 = \frac{1}{NL} \text{Re} \sum_j \lim_{t \rightarrow 0} \langle \psi_{ja,1}(t) \chi_{ja}(0) \rangle \quad (59)$$

$$= \gamma \int \frac{d\omega}{\pi} f(\omega) \text{Im} [G_{\psi\chi}(\omega + i\eta) - G_{\psi\chi}(\omega - i\eta)].$$

We can use equation of motion (EoM) to calculate the mixed function but first, better write $\psi_{ja,1}$ in momentum space:

$$G_{\psi\chi}(\tau) \equiv \langle -T c_{ja,1}(\tau) \chi_{ja} \rangle = \sum_k \langle -T c_{ja,1k}(\tau) \chi_{ja} \rangle. \quad (60)$$

Note that $c_{ja,1k}$ refers to $\alpha = 1$ and k is the electron momentum. EoM gives

$$\begin{aligned} -\partial_\tau G_{c\chi}(\tau) &= \langle -T[c_{ja1,k}, H]_\tau \chi_{ja} \rangle \\ &= \langle -T\{\epsilon_k c_{ja1,k}(\tau) + \bar{b}'_1 \chi_{ja}^\dagger(\tau)\} \chi_{ja} \rangle, \end{aligned} \quad (61)$$

or

$$(-\partial_\tau - \epsilon_k) G_{c\chi}(\tau) = \bar{b}'_1 \langle -T \chi_{ja}^\dagger(\tau) \chi_{ja} \rangle, \quad (62)$$

which after momentum summation leads to

$$G_{\psi\chi}(\tau) = \bar{b}'_1 \sum_k g_k(\tau) * \langle -T \chi_{ja}^\dagger(\tau) \chi_{ja} \rangle. \quad (63)$$

To find the Fourier transform of the last term, note that fermionic Lehmann representation of $\langle -T \chi_j(\tau) \chi_j^\dagger \rangle$ is

$$G(i\omega_n) = -\frac{1}{Z} \sum_{mn} |\langle n | \chi | m \rangle|^2 \frac{e^{-\beta E_n} + e^{-\beta E_m}}{i\omega_n + E_n - E_m} \quad (64)$$

Therefore, $\chi \rightarrow \chi^\dagger$ corresponds to $n \leftrightarrow m$ and $G(i\omega_n) \rightarrow -G(-i\omega_n)$. So,

$$G_{\psi\chi}^R(\omega) = -\bar{b}'_1 g^R(\omega) G_\chi^A(-\omega). \quad (65)$$

Plugging this into Eq. (59) we find

$$\lambda - 2\Delta = -\gamma \int \frac{d\omega}{\pi} f(\omega) [g_{c1}''(\omega) G_\chi'(-\omega) - g_{c1}'(\omega) G_\chi''(-\omega)], \quad (66)$$

and of course $n_B(\lambda) = s - m$ where we defined the magnetization, $m \equiv \bar{b}_1'^2$. In the case of an isolated spin, it condensed whenever its energy $\lambda = 0$ becomes zero. The above equation is generalization of that formula to the Kondo case. The self-energy of χ is modified

$$\Sigma_\chi(\tau) = \frac{N-1}{N} g_c(-\tau) G_{B,\alpha \neq 1}(\tau) - \bar{b}_1'^2 g_c(-\tau), \quad (67)$$

so that in large- N we have

$$\Sigma_\chi(\omega + i\eta) = \Sigma_\chi^{\text{old}}(\omega + i\eta) - m g_c(-\omega - i\eta) \quad (68)$$

and the self-energy of the bosons is not modified.